ELSEVIER

Journal of Alloys and Compounds 444–445 (2007) 673–676

Journal of ALLOYS AND COMPOUNDS

www.elsevier.com/locate/jallcom

Anhydrous photochemical reduction of well-defined uranyl(VI) complexes

Paul B. Duval *, Shanmugaperumal Kannan

Department of Chemistry, University of Missouri-Columbia, 601 S. College Avenue, Columbia, MO 65211, United States

Received 30 June 2006; received in revised form 31 October 2006; accepted 1 November 2006
Available online 13 December 2006

Abstract

The photochemical reactivity of well-defined cationic uranyl(VI) complexes is presented under non-aqueous conditions employing systematic control over variable experimental conditions, with a focus on structural and electronic characterization of the products. The results offer mechanistic insight into alternate pathways of dioxo activation during the photochemical reduction of uranyl(VI) that are operable only under anhydrous conditions.

Keywords: Actinide alloys and compounds; Chemical synthesis; X-ray diffraction

1. Introduction

Reports detailing the activation of the normally robust uranyl(VI) dioxo group are rare and confined primarily to two types of processes, both of which are accompanied by significant alteration of the uranium coordination sphere. The first involves nucleophilic interactions of the dioxo group to various Lewis acids in electron-rich uranyl(VI) complexes [1,2], culminating in some instances in oxo-atom abstraction with substrates or functional groups that are particularly oxophilic [3–5]. This mode of activation may or may not be accompanied by uranium reduction.

The other means by which the dioxo unit is disrupted occurs during the reduction of uranyl(VI) to uranium(IV) [6–8], with the contrasting solubility between these two species imparting considerable consequences in uranium environmental and reprocessing chemistry [9]. Applications directed toward the remediation and reprocessing of nuclear waste have focused on various redox strategies to immobilize soluble UO_2^{2+} to insoluble U(IV), employing microorganisms (i.e., sulfate-reducing bacteria) or chemical, electrochemical or photochemical reduction methods [10]. The photochemical reduction of uranyl(VI) has been extensively studied with a number of reductants under a variety of experimental conditions [11,12].

The photochemical reduction of uranyl(VI) with alcohols is considered to proceed through two steps, entailing a one-electron reduction to uranyl(V) followed by the disproportionation of the unstable UO_2^{+} intermediate, although mechanistic details remain remarkably sparse [13]. While the redox instability of the UO_2^{+} ion hampers study of this elusive oxidation state, details are even murkier surrounding the transformation of the dioxo group and the identity of the final uranium(IV) species, as well as the complex interplay of the bimolecular disproportionation reaction. Although these reactions have been evaluated under a variety of experimental conditions, perhaps the most important factor that influences this redox chemistry, the coordination sphere of the precursor uranyl species, has largely been ignored.

It is in this context that the photochemical reactivity of well-defined cationic uranyl(VI) complexes coordinated solely by bulky electron-withdrawing phosphine-oxide ligands is presented under non-aqueous conditions, with a focus on structural and electronic characterization of the products. The results offer mechanistic insight into alternate pathways of dioxo activation during the photochemical reduction of uranyl(VI).

2. Results and discussion

We are currently exploring the photochemical reduction of well-defined cationic uranyl(VI) complexes coordinated by bulky neutral electron-withdrawing ligands. In addition to possessing the steric bulk and electronic compatibility for favorable equatorial coordination, the electron-withdrawing aryl sub-

* Corresponding author. Tel.: +1 573 882 1735; fax: +1 573 882 2754.
E-mail address: duvalp@missouri.edu (P.B. Duval).

0925-8388/$ – see front matter © 2006 Elsevier B.V. All rights reserved.
doi:10.1016/j.jallcom.2006.11.035

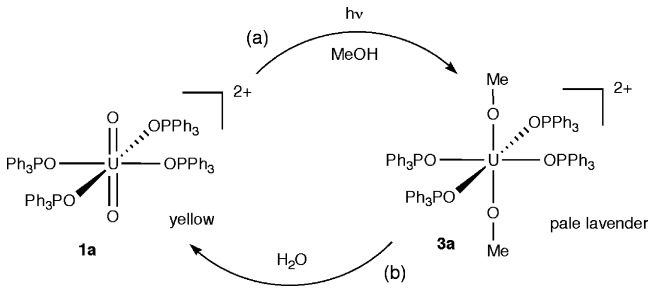

Scheme 1.

stituents of the hard phosphine oxide ligands combine with the positive charge of the uranyl(VI) complexes to lower the energy of the uranium valence orbitals, rendering the reduced uranyl(V) intermediate less prone to re-oxidation (accordingly, reactions are conducted under anaerobic conditions) and disproportionation due to stronger metal–ligand bonding and steric congestion.

From these studies we have observed that the identity of the counter-anion can dramatically influence the photochemical pathway. For example, the photoreduction of $[UO_2(OPPh_3)_2][OTf]_2$ (**1a**) [14] with either methanol or diethyl ether leads to uranium(IV) alkoxide complexes with unprecedented retention of the equatorial coordination plane as the axial dioxo unit is replaced by alkoxide groups. The reaction of **1a** with methanol to yield *trans*-$[U(OMe)_2(OPPh_3)_4][OTf]_2$ (**3a**) is outlined in Scheme 1 [15]. Methanol serves as both the reductant (relying on the strong photo-oxidative strength of the $^*UO_2^{2+}$ ion) and the source of methoxide ligands, the latter through hydrolysis of the axial dioxo group. Similarly, exposing a solution of **1a** in diethyl/ether to UV light generates the corresponding ethoxide derivative *trans*-$[U(OEt)_2(OPPh_3)_4][OTf]_2$ (**3b**). In this instance photolysis of diethyl ether produces ethanol, thus yielding the ethoxide ligands through the analogous mechanism as obtained for **3a**.

Single crystals of **3a** and **3b** suitable for X-ray crystallography were obtained from acetonitrile, although disorder precluded analysis of **3b** beyond connectivity, which is similar to that detailed for **3a** below. A thermal ellipsoid drawing of the cation of **3a** is shown in Fig. 1. A *trans*-octahedral UX_2L_4 geometry is observed for the uranium center, consisting of two axial methoxide groups and four neutral $OPPh_3$ ligands occupying the equatorial sites, with minimal deviation observed from idealized tetragonal geometry. Thus the solid-state structure of **3a** closely resembles that of the precursor **1a** except for the replacement of methoxide groups for the dioxo unit in the axial positions [16]. The U(1)–O(3) bond distance of 2.0575(5) Å is comparable to the terminal U–O bonds found in other structurally characterized uranium methoxide complexes [17], while the open U(1)–O(3)–C(13) bond angle of 180.000(1)° is typical of uranium alkoxide complexes and may also reflect enhanced π-bonding analogous to the favorable bonding interactions that reinforce the *trans*-dioxo geometry. The U–O bond distances (2.330(3) Å) to the $OPPh_3$ ligands are similar to those reported to **1a** and within the normal range for uranium complexes coordinated by these ligands.

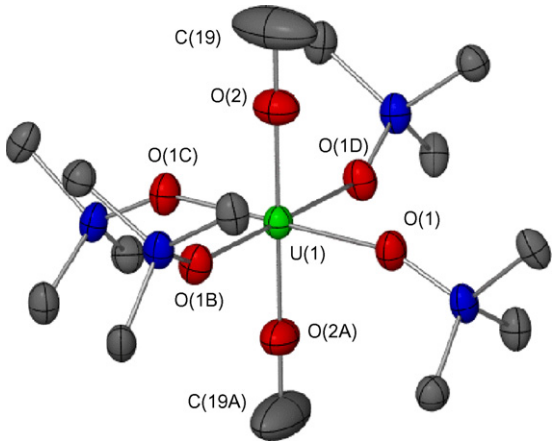

Fig. 1. Thermal ellipsoid drawing of the cation of **3a**, with displacement ellipsoids shown at 50% probability. For clarity only the *ipso* carbon atoms of the phenyl rings are omitted shown. Selected bond lengths (Å) and bond angles (°): U–O(1), 2.330(3); U–O(2), 2.057(5); O(1)–P(1), 1.522(3); O(2)–C(19), 1.416(14); O(2)–U–O(2A), 180.0; O(1)–U–O(2), 89.94(7); U–O(1)–C(19), 180.000(1); U–O(1)–P(1), 150.26(19).

Spectroscopic data suggest that a similar result is obtained for the related derivative $[UO_2(dppmo)_2(OPPh_3)][OTf]_2$ (**2a**; dppmo = $Ph_2P(O)CH_2P(O)Ph_2$). However, the same reaction conducted with the BF_4^- analogue $[UO_2(dppmo)_2(OPPh_3)][BF_4]_2$ (**2b**) instead produces the cationic uranium(IV) fluoride complex $[UO_2F_2(dppmo)_3][BF_4]_2$ (**4**). This reaction proceeds through two separate sequences of fluoride abstraction from BF_4^- anions by a uranium center (Scheme 2) [18]. The first occurs prior to photochemical reduction of **2b** and forms the fluoride-bridged dinuclear uranyl(VI) complex $[(UO_2(dppmo)_2)_2(\mu\text{-}F)][BF_4]_3$, followed by a second fluoride abstraction during photolysis to give **4**. The accumulation of three dppmo groups and two fluoro ligands in forming **4** from the precursor **2b** reflects the extensive ligand distribution that typically accommodates disproportionation of the labile uranyl(V) intermediate, a feature that is notably absent in the transformation of **1a** to **3**.

Single crystals suitable for X-ray crystallography were obtained for **4** (Fig. 2). The eight-coordinate uranium(IV) center in the cation contains three chelating dppmo ligands and two terminal fluorides in a geometry that approximates a distorted dodecahedron, with F(1), O(2), O(3) and O(4) comprising a roughly coplanar trapezoid perpendicular to another trapezoid consisting of F(2), O(1), O(5) and O(6). Allowing for conformational flexibility in the chelating dppmo ligands the cation in **4**

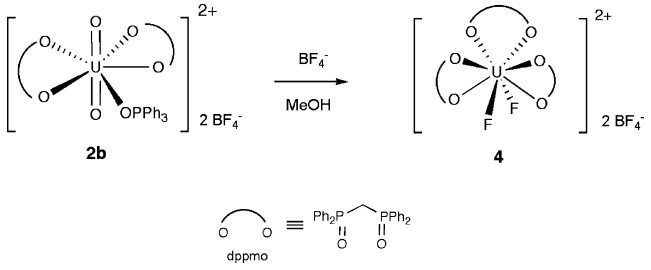

Scheme 2.

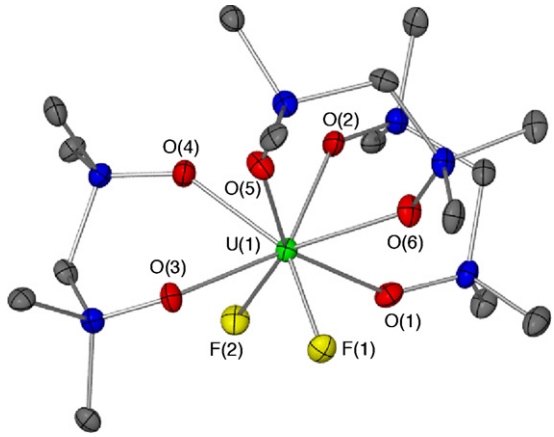

Fig. 2. Thermal ellipsoid drawing of the cation of **4** showing the atom-labeling scheme used in the tables. Displacement ellipsoids are shown at 50% probability. For clarity only the *ipso* carbon atoms of the phenyl rings are omitted shown. Selected bond lengths (Å) and bond angles (°): U–O(1), 2.441(3); U–O(2), 2.386(4); U–O(3), 2.465(3); U–O(4), 2.407(3); U–O(5), 2.379(3); U–O(6), 2.503(3); U–F(1), 2.123(3); U–F(1), 2.131(3); F(1)–U(1)–F(2), 90.07(12); O(1)–U–O(2), 72.17(12); O(3)–U–O(4), 74.50(12); O(5)–U–O(6), 70.92(12).

exhibits approximate C_s point group symmetry with the F–U–F unit defining a mirror plane.

The U–F bond distances of 2.123(3) Å for U(1)–F(1) and 2.131(3) Å for U(1)–F(2) are similar to that of 2.106(12) Å in Cp_3UF, which represents the only other structurally characterized uranium(IV) complex possessing a terminal U–F bond [19]. The fairly wide range in U–O bond distances in **4**, from 2.379(3) to 2.503(3) Å, is reflected in alternating short/long distances within individual dppmo ligands. Other structural features, including the dppmo O–U–O bite angles (between 70.92(12) and 74.50(12)°) are within the normal range.

It is worth noting that both **3** and **4** are reversibly oxidized to uranyl(VI) species through hydrolysis (for example, Scheme 1(a)), by adding trace amounts of water to acetonitrile solutions under anaerobic conditions.

3. Experimental

3.1. General considerations

Unless otherwise stated all manipulations were conducted under an inert atmosphere of dry, oxygen-free dinitrogen in a MBraun Labmaster 130 glovebox equipped with a MB 20G purification system or in standard Schlenk-type glassware on a dual vacuum/dinitrogen line. Toluene, diethyl ether and hexanes (Fisher) were dried by passage through an MBraun solvent purification system (MB-SPS) consisting of one column of activated alumina and one column of activated copper catalyst (toluene, hexanes), or two columns of alumina (diethyl ether). Tetrahydrofuran (THF) was distilled over sodium benzophenone ketyl. Anhydrous methanol and triphenylphosphine-oxide (Aldrich) were used as received. Photochemical reactions were conducted with stirring in an ace glass reactor assembly operating with output from a 450 W Hg vapor lamp in a quartz immersion well, in an enclosed cabinet. ^{1}H spectra (referenced to non-deuterated impurity in the solvent) were recorded on a Bruker AMX-250 or -300 spectrometer. $^{31}P\{^1H\}$ NMR spectra (referenced to external 85% H_3PO_4) were run at 101.25 MHz on the AMX-250 instrument. ^{19}F NMR spectra (referenced to external $CFCl_3$) were run at 235.36 MHz on the AMX-250 instrument. Chemicals shifts are reported in ppm and all coupling constants are reported in Hertz unless otherwise noted. Infrared spectra were obtained as a mull in immersion oil pressed between KBr plates on a Thermo Nicolet Nexus 670 FT-IR spectrometer. UV–vis spectra were obtained as THF and acetonitrile solutions on a Hewlett-Packard 8452A diode-array spectrophotometer. Elemental analyses were performed by Desert Analytics.

3.2. Synthesis of trans-$[U(OMe)_2(OPPh_3)_4][OTf]_2$ (**3a**)

A methanol solution (5 mL) of **1a** (416 mg, 0.25 mmol) was irradiated under a UV lamp for 5 h, during which the yellow solution turned pale lavender. The reaction mixture was filtered and the filtrate evaporated to 1 mL and layered with 5 mL of ether. Colorless crystals obtained at −30 °C were washed with ether and dried (360 mg, 78%). ^{1}H NMR (300 MHz, CD_3CN, 23 °C, TMS) (ppm): δ −5.0 (br s, 24H, *o*-C_6H_5), 5.4 (br s, 24H, *m*-C_6H_5), 7.4 (m, 12H, *p*-C_6H_5), 170 (br s, 6H, OCH_3); $^{31}P\{^1H\}$ NMR (121.5 MHz, CD_3CN, 23 °C, H_3PO_4) (ppm): δ −88; ^{19}F NMR (25 °C, CD_3CN): δ −79.6 (s, CF_3SO_3); elemental analysis (%) calcd. for $C_{76}H_{66}F_6O_{12}P_4S_2U$: C, 53.34; H, 3.89. Found: C, 53.77; H, 4.31.

3.3. Synthesis of trans-$[U(OEt)_2(OPPh_3)_4][OTf]_2$ (**3b**)

Diethyl ether (2 mL) was added to an acetonitrile solution (5 mL) of **1a** (500 mg, 0.30 mmol) and this solution was exposed to UV light for 24 h. The resulting pale green solution was evaporated to dryness and the residue extracted with 2 mL of acetonitrile and filtered. The filtrate was layered with 10 mL of ether, from which colorless crystals were obtained at −35 °C, washed with ether and dried (350 mg, 69%). ^{1}H NMR (300 MHz, CD_3CN, 23 °C, TMS) (ppm): δ −8.1 (br s, 24H, *o*-C_6H_5), 4.6 (br s, 24H, *m*-C_6H_5), 6.9 (m, 12H, *p*-C_6H_5), 75.3 (br s, 6H, OCH_2CH_3), 180 (br s, 4H, OCH_2CH_3); $^{31}P\{^1H\}$ NMR (121.5 MHz, $CDCl_3$, 23 °C, H_3PO_4) (ppm): δ −91; ^{19}F NMR (25 °C, CD_3CN): δ −79.4 (s, CF_3SO_3).

3.4. Synthesis of $[UF_2(dppmo)_3][BF_4]_2$ (**4**)

A pale yellow solution of **2b** (450 mg, 0.33 mmol) in 25 mL methanol was exposed to UV light for 3 h, and the resulting blue solution was filtered to remove some insoluble yellow material. The addition of ether to the clear filtrate produced a light blue powder that was filtered, washed with ether and dried. Recrystallization from CH_3CN/diethyl ether yielded a blue-green crystalline solid. Yield: 212 mg (37%). ^{1}H NMR (25 °C, CD_3CN): δ −12.7 (br, 6H, PCH_2P), 6.1 (br, 24H, C_6H_5), 6.7 (br t, 12H, C_6H_5), 7.4 (br, 24H, C_6H_5). $^{31}P\{^1H\}$ NMR (25 °C, CD_3CN): δ −81.5 (s). ^{19}F NMR (25 °C, CD_3CN): δ −152 (s, BF_4). Anal. calcd. for $C_{75}H_{66}B_2F_{10}O_6P_6U$: C, 53.03; H, 3.96. Found: C, 52.86; H, 4.26.

3.5. X-ray crystallographic data

Single crystals of suitable quality for X-ray analysis for **3a** and **4**, respectively, were obtained from acetonitrile (**3a**) and layered CH_3CN/diethyl ether (**4**). Single crystals placed in degassed hydrocarbon oil were mounted on a glass fiber. Intensity data were obtained at −100 °C on a Bruker SMART CCD area detector system using the ω-scan technique with Mo Kα radiation from a graphite monochromator. Intensities were corrected for Lorentz and polarization effects. Equivalent reflections were merged, and absorption corrections were made using the multi-scan method. The structures were solved by direct methods with full-matrix least-squares refinement, using the SHELX package. All non-hydrogen atoms were refined with anisotropic thermal parameters. The hydrogen atoms were placed at calculated positions and included in the refinement using a riding model, with fixed isotropic U.

Acknowledgements

This work was financially supported by the American Chemical Society Petroleum Research Fund, the Missouri University Research Reactor, and the University of Missouri Research Board.

References

[1] M.J. Sarsfield, M. Helliwell, J. Am. Chem. Soc. 126 (1036) (2004).
[2] M.P. Wilkerson, C.J. Burns, H.J. Dewey, et al., Inorg. Chem. 39 (5277) (2000).
[3] C.J. Burns, A.P. Sattelberger, Inorg. Chem. 27 (3692) (1988).
[4] P.C. Levard, D. Rinaldo, M. Nierlich, Dalton Trans. 829 (2002).
[5] P.B. Duval, C.J. Burns, W.E. Buschmann, et al., Inorg. Chem. 40 (5491) (2001).
[6] J.-C. Berthet, P. Thuéry, M. Ephritikhine, Chem. Commun. 3415 (2005).
[7] A.C. Bean, T.A. Sullens, W. Runde, et al., Inorg. Chem. 42 (2628) (2003).
[8] C.L. Cahill, P.C. Burns, Inorg. Chem. 40 (1347) (2001).
[9] J.J. Katz, G.T. Seaborg, L.R. Morss, The Chemistry of the Actinide Elements, Chapman and Hall, London, 1986.
[10] R.B. Payne, D.M. Gentry, B.J. Rapp-Giles, et al., Appl. Environ. Microbiol. 68 (3129) (2002).
[11] T.M. McCleskey, T.M. Foreman, E.E. Hallman, et al., Environ. Sci. Technol. 35 (547) (2001).
[12] C.J. Dodge, A.J. Francis, Environ. Sci. Technol. 36 (2094) (2002).
[13] C.P. Baird, T.J. Kemp, Prog. React. Kinet. 22 (87) (1997).
[14] J.-C. Berthet, M. Nierlich, M. Ephritikhine, Dalton Trans. 2814 (2004).
[15] S. Kannan, A.E. Vaughn, E.M. Weis, et al., J. Am. Chem. Soc. 128 (14024) (2006).
[16] J.-C. Berthet, M. Nierlich, M. Ephritikhine, Angew. Chem., Int. Ed. 42 (1952) (2003).
[17] L. Karmazin, M. Mazzanti, J. Pécaut, Inorg. Chem. 42 (5900) (2003).
[18] S. Kannan, M.A. Moody, C.L. Barnes, et al., Inorg. Chem. 45 (9206) (2006).
[19] R.R. Ryan, R.A. Penneman, B. Kanellapulos, J. Am. Chem. Soc. 97 (4258) (1975).